

# Homology modeling and SAR analysis of *Schistosoma japonicum* cathepsin D (SjCD) with statin inhibitors identify a unique active site steric barrier with potential for the design of specific inhibitors

Conor R. Caffrey<sup>1</sup>, Lenka Placha<sup>2</sup>, Cyril Barinka<sup>2</sup>, Martin Hradilek<sup>2</sup>, Jiří Dostál<sup>2</sup>, Mohammed Sajid<sup>1</sup>, James H. McKerrow<sup>1</sup>, Pavel Majer<sup>3</sup>, Jan Konvalinka<sup>2</sup> and Jiří Vondrášek<sup>2,4,\*</sup>

<sup>1</sup>Sandler Center for Basic Research in Parasitic Diseases, University of California at San Francisco, Box 0511, San Francisco, CA 94143, USA

<sup>2</sup>Institute of Organic Chemistry and Biochemistry, Academy of Sciences of the Czech Republic, Flemingovo n. 2, 166 10 Praha 6, Czech Republic

<sup>3</sup>Guilford Pharmaceuticals Inc., 6611 Tributary Street, Baltimore, MD 21224, USA

<sup>4</sup>Center for Biomolecules and Complex Molecular Systems, Institute of Organic Chemistry and Biochemistry, Academy of Sciences of the Czech Republic, Flemingovo n. 2, 166 10 Praha 6, Czech Republic

\*Corresponding author  
e-mail: jirka@uochb.cas.cz

## Abstract

Proteases that digest the blood-meal of the parasitic fluke *Schistosoma* are potential targets for therapy of schistosomiasis, a disease of chronic morbidity in humans. We generated a three-dimensional model of the cathepsin D target protease of *Schistosoma japonicum* (SjCD) utilizing the crystal structure of human cathepsin D (huCD) in complex with pepstatin as template. A homology model was also generated for the related secreted aspartic protease 2 (SAP2) of the pathogenic yeast, *Candida albicans*. An initial panel of seven statin inhibitors, originally designed for huCD [Majer et al., Protein Sci. 6 (1997), pp. 1458–1466], was tested against the two pathogen proteases. One inhibitor showed poor reactivity with SjCD. Examination of the SjCD active-site cleft revealed that the poor inhibition was due to a unique steric barrier situated between the S2 and S4 subsites. An *in silico* screen of 20 potential statin scaffolds with the SjCD model and incorporating the steric barrier constraint was performed. Four inhibitors (SJ1–SJ4) were eventually synthesized and tested with SjCD, bovine CD and SAP2. Of these, SJ2 and SJ3 proved moderately more specific for SjCD over bovine CD, with IC<sub>50</sub> values of 15 and 60 nM, respectively. The unique steric barrier identified here provides a structural focus for further development of more specific SjCD inhibitors.

**Keywords:** active site; aspartyl protease; *Candida*; drug design; parasite.

## Introduction

Schistosomiasis, caused by parasitic bloodflukes of the genus *Schistosoma*, is of serious public health concern in 74 tropical and sub-tropical countries. More than 200 million people are infected, with 20 million suffering from serious disease (Chitsulo et al., 2004). Adult worms reside within the blood vessels of the intestine and bladder, and their eggs cause morbidity associated with a progressive, immunopathological reaction in various tissues including the liver and intestine (Pearce and MacDonald, 2002).

Schistosomes feed on blood proteins, including hemoglobin, and express a range of gut-associated proteases to facilitate digestion. The proteases thought to be directly involved in this process include orthologs of the mammalian cysteine proteases, cathepsins B and L, and the aspartic protease, cathepsin D (see Caffrey et al., 2004 for a review). Because of their critical function in nutrition, therefore, such proteases are considered potential targets for chemotherapeutic intervention (Caffrey et al., 2004) and, indeed, the cysteine proteases have been demonstrated as such (Wasilewski et al., 1996).

The fully processed cathepsin D of the Asian blood-fluke *Schistosoma japonicum* (SjCD; accession number L41346, Becker et al., 1995, modified as U90750) shares 57.2% identity with human cathepsin D (huCD). Like this enzyme, SjCD displays an acid pH optimum (Caffrey et al., 1998; Brindley et al., 2001) and preferentially hydrolyzes bonds between two hydrophobic residues (Brindley et al., 2001). However, the preferential cleavage sites in human hemoglobin for SjCD and huCD differ (Brindley et al., 2001), suggesting significant topographical differences between the active-site clefts of both enzymes. Such differences might be exploited in the rational design of novel and selective drugs to treat schistosomiasis. In the absence of crystal structures of schistosome CDs, comparative molecular modeling using the crystal structure of huCD [Protein Data Bank (PDB) ID: 1LYB; Baldwin et al., 1993] has been applied to explain active site differences between parasite and human orthologs (Brinkworth et al., 2001; Silva et al., 2002). Thus far, however, no attempt has been made to screen, design or test small-molecule inhibitors of schistosome CDs either using structure-activity relationship (SAR) studies with a homology model or otherwise.

For this report, we generated a homology model of SjCD in complex with pepstatin and compared the active-site amino acid composition and topography with both huCD and the related protease, secreted aspartic protease 2 (SAP2), from the pathogenic fungus *Candida*

*albicans*. SAP2, in addition to its usefulness here as a comparative model, is a potential drug target in its own right (Bein et al., 2002). Furthermore, as a first attempt to design inhibitors with greater specificity for SjCD, we incorporated the SjCD model in a SAR study to screen a panel of statin-based CD inhibitors both *in silico* and *in vitro*. The SAR approach revealed a novel topographical steric barrier within the active-site cleft of SjCD not present in either huCD or SAP2. Finally, the presence of the SjCD steric barrier was incorporated into the design and eventual testing of second-generation inhibitors for increased specificity to SjCD.

## Results

### Characterization and comparison of structural models

A CLUSTAL W (Higgins et al., 1994) sequence alignment of SjCD, huCD and SAP2 (Figure 1) highlights the conservation of sequences between the three proteases. All models, optimized by the same computational protocol (Table 1), were compared with the crystal structure of huCD in complex with pepstatin. The binding cavities of SjCD, SAP2, and huCD (Figure 2) were further characterized with respect to the contact of their amino acid residues with pepstatin in the S4-S2' subsites. Connolly contact surface plots between enzyme and inhibitor were also generated and gaps between enzyme and inhibitor were determined. We included all atoms within the distance limit of 4.5 Å between pepstatin and the modeled proteases.

### SjCD and SAP2 theoretical models in complex with pepstatin A and their comparison with the huCD-pepstatin A complex

**SjCD** The modeled structure of SjCD (Figure 3) differs from that of huCD mainly in the active site loops. The greatest deviations were located around positions B120–B130, B139–B152, B252–B269, B276–B283, B310–B320 and B292–B303 (where B is the chain identification of the SjCD model based on huCD). These changes would partially account for the different subsite specificities measured (see green arrows in Figure 3). The root mean square deviation (RMSD) of the C $\alpha$  ( $\alpha$  carbon) chain of huCD with the model of SjCD was 2.06 Å. Our structural model was also compared with that published by Brinkworth et al. (2001). Coordinates of their model are not available, however, so we compared only the composition of the subsites obtained here with those described in Table 1 of their report. The substantial agreement found confirms the structural reliability of both independently constructed models.

Although a similar binding mode of the pepstatin backbone is seen in all the proteases studied, the geometry of the N-terminal isovaleric acid of pepstatin in SjCD (occupying the S3 and S4 subsites) differs from those in SAP2 and huCD. Also, the S3 and S4 subsites in both huCD and SAP2 are more open. SjCD lacks hydrogen bonding in the narrow S3 subsite, probably due to a lack of flexibility of pepstatin. In the S1 and S1' subsites, SjCD

binds pepstatin extensively and the character of this binding is mainly hydrophobic.

**SAP2** The major difference in the structural model of SAP2 compared to huCD (Figure 3) is localized around the active site loop residues A242–A253 (where A is the chain identification of the SAP2 model). The active site of SAP2 is clearly more open (see red arrows in Figure 3). The isovaleric acid of pepstatin is oriented towards the wide SAP2 S4 subsite, which is the widest of the three proteases. Towards the C-terminus of pepstatin and unlike the extensive contacts in SjCD, the inhibitor offers no contacts with the S1' subsite residues of SAP2 within the limit measured. Also, at the S2' subsite, SAP2 seems to bind non-specifically and the strength of the interactions is almost negligible. This is in contrast to the SjCD model, in which both S1' and S2' control placement of the inhibitor terminus. Overall, the binding modes of pepstatin in huCD are more similar to those of SAP2 than SjCD.

Based on the analyses of subsites (Figure 2), it is clear that SjCD can accommodate hydrophobic over polar residues in S1 and S1'. In contrast, S3 shows no obvious selectivity. For S2, SAP2 requires a bulky residue, whereas smaller residues are preferred in huCD and SjCD.

### Comparison of SAR with a panel of statin inhibitors

Inhibition data for a panel of seven statin inhibitors tested with SjCD, SAP2, and huCD are presented in Table 2. The data for huCD are taken from Majer et al. (1997). All inhibitors except P7 were potent against SjCD. Compared with P2, the prominent structural difference in P7 is the bridging of the P1 and P3 residues. This bridge is tolerated by both huCD and SAP2, but rejected by SjCD, resulting in an IC<sub>50</sub> value three orders of magnitude greater than those of the other inhibitors. There are two possible explanations for the lack of inhibition by P7. First, the bridge between P1 and P3 is mostly polar and, therefore, not completely compatible with the less polar binding sites. Alternatively, the bridge may require plasticity of the active site, or at least a large enough cavity. As shown in Figure 4, SjCD has an obvious steric barrier between the S2, S3, and S4 subsites corresponding to placement of the P1 and P3 residues. In contrast, the active site subsites of huCD and SAP2 lack distinctive borders or contours and are more cylindrical in shape. The steric barrier in SjCD is composed mainly of the side chains of Met 224 and Phe 120.

### Second-generation statin inhibitors of SjCD

Using the SjCD-pepstatin model and analyses of other pepstatin-enzyme complexes (Table 3 and Table 4), we attempted to design more specific statin inhibitors of SjCD. The newly identified steric barrier of SjCD was taken into account with respect to the conformational properties of the new inhibitors. Also, the design reflected the following criteria of compatibility between the protease and ligand: (a) geometrical compatibility, (b) environment compatibility, (c) length requirements, and (d) ligand flexibility. It is known that the binding sites of aspartic proteases show great plasticity and, in principle, can accommodate a wide range of substrates and inhibitors

```

      1      10      20      30      40      50      60
SjCD  VEPRPEYLKNYLDAQYYGDITIGTPPQTFVVFDTGSSNLWVP--SKHCSYFDIA-----
huCD  -GPIPEVLKNYMDAQYYGEIGIGTPPQCFTVVFDTGSSNLWVP--SIHCKLLDIA-----
SAP2  -QAVPVTLHN-EQVTYAADITVGSNNQKLNVIIVDTGSSDLWVPDWNVCQVQVTSQDTADF
      . * *:* :. * .:* :*: * :*.*****:**** . *.

      61      70      80      90      100     110     120
SjCD  CLLHRKYDSSKSTTYVPNGTDFSIRYGTGSLG-GFLSTDSL-----QLGSLGVK
huCD  CWIHHKYNSDKSSTYVKNGTDFDIHYGSGSLG-GYLSQDTVSVPCQSASSASALGGVKVE
SAP2  CKQKGTYPDPSGSSASQDLNTPFKIGYDGGSSSQGTLYKDTVG-----FGGVS IK
      * :.*:..*:: . * *.* ** * * * * * * * *:: :*: :.

      121     130     140     150     160     170     180
SjCD  GQTFGEATKQPGLVFMVMAKFDGILGMAYPSLAVGGVTP-VFVNMIKQGVVDSPVFSFYLS
huCD  RQVFGQATKQPGITFIAAKFDGILGMAYPRISVNNVLP-VFDNLMQKQLVDQNI FSYLS
SAP2  NQVLADVDS---TSIDQ---GILGVGYKTNEAGGSYDNVPTLKKQGVIAKNAYSLYLN
      *.:.:. . : ****:.* ... * .: :* :. . :*:*.

      181     190     200     210     220     230     240
SjCD  RNITNVLGGELMIGGIDDKYTGEEINYNLTKESYWLFKMDNLTISD-LSICTDGCQAIA
huCD  RDPDAQPGGELMLGGTDSKYKGSLSYLNVRKAYWQVHLDQVEVASGLTLCKEGCEAIV
SAP2  -SPDAATG-QIIFGGVDNAKYSGLIALPVTSDRELRLISLGSVEVSG-KTINTDNDVLL
      . * :.:** *. *.*: : :* . . :.: :. :. :. :.

      241     250     260     270     280     290     300
SjCD  DTGTSMIAGPTDEVKQINQKLGATHLPGGIYTVSCDVINNLPSIDFVINGKHMTPLEPTY
huCD  DTGTSMLVGPVDEVRELQKAIGAVPLIQGEYMIPECEKVSTLPAITLKLGGKGYKLSPEDY
SAP2  DSGTTITYLQQLADQIIKAFNGKLTQDSNGNSFYEVDCNLSGDDVVFNFNSKNAKISVPAS
      *:***: * . :. : :. . : *.. . * .:..

      301     310     320     330     340     350     360
SjCD  IMKVSKLGSEICLTGFIGMDLPRKK--LWILGDVFIGKFYTI FDMGKNRVGFAKAVKPD
huCD  TLKVSQAGKTLCLSGFMGMDIPPSGPLWILGDVFIGRYTYVFDNRNVRVGFABEARL--
SAP2  EFAASLQGGDGPYDKCQLLFDVND--ANILGDNFLRSAYIVYDLDDNEISLAQVKYTS
      : .* *. . : : . **** * : * :.* ..*.:*:.

      361     370     380     390     400
SjCD  SYHHTKVYSPMLRLFPAQSI PKVAPKSPNGVFAFSKLLHDAN
huCD  -----
SAP2  SSISALT-----

```

**Figure 1** Multiple sequence alignment of SjCD (accession no. AAB63357), huCD (NP\_001900) and SAP2 (P28871) by CLUSTAL W (Higgins et al., 1994).

Asterisks indicate identity across all three proteases for a given amino acid residue; colons indicate similarity in hydrophobicity for two positions, and a period indicates similarity in charge character for two positions. The active site triads are highlighted in grey.

**Table 1** The minimization protocol for the models of SjCD, huCD and SAP2 in complex with pepstatin.

Molecule	Fixed	Number of iterations	Convergency criterion	Algorithm	Convergency criterion reached
SjCD	Heavy atoms	1000	0.05	Steepest descent	no
SjCD	Backbone	1000	0.05	Steepest descent	no
SjCD	Backbone	1500	0.05	Steepest descent	no
SjCD	Backbone	5000	0.01	Steepest descent	no
SjCD	Heavy atoms	1000	0.001	Steepest descent	no
SjCD	Backbone	1500	0.001	Conjugated gradient	yes
SjCD	None	5000	0.001	Conjugated gradient	yes
HuCD	None	5000	0.001	Conjugated gradient	yes
SAP2	Heavy atoms	1000	0.05	Steepest descent	no
SAP2	Backbone	5000	0.001	Conjugated gradient	yes
SAP2	None	5000	0.001	Conjugated gradient	yes



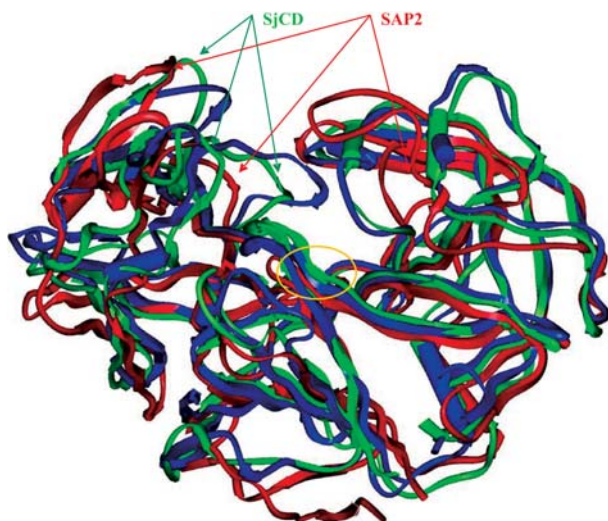


**Figure 3** Superimposition of huCD (blue), SjCD (green) and SAP2 (red) by their C $\alpha$  atoms in ribbon representation with secondary structure elements.

Green and red arrows point to regions where both proteases show significant differences at the active site from huCD (see text for details). The yellow ellipse indicates the region where active site residues are located.

that can differ in length, type, and composition (Vondrasek and Wlodawer, 1998). Therefore, our study focused on finding a reasonable scaffold with greater specificity for SjCD over huCD. The statin scaffold is the most straightforward option for the design, satisfying the criteria of large conformational flexibility and selectivity for aspartic proteases.

To allow for a direct comparison of the potency of the four new inhibitors with SjCD, bovCD, and SAP2, the same peptide substrate, 2-aminobenzoyl-Ile-Glu-Phe-nitroPhe-Arg-Leu-NH<sub>2</sub>, was used (Table 5). Two of the four inhibitors, SJ2 and SJ3, were moderately more specific for SjCD than bovCD. Also, SJ2 and SJ4 were more effective against SjCD than SAP2. Detailed analyses of the binding modes of these second-generation compounds did not reveal any substantial changes in binding nature. All inhibitors were also docked into huCD structures for comparison with the modeling template. This revealed that the binding of the new inhibitors is more or less uniform in all three enzymes studied.

## Discussion

Adult schistosome parasites digest blood proteins, including hemoglobin, for their nutritional and reproductive requirements. Alimentary cysteine proteases, orthologous to mammalian cathepsins B and L, and an

**Table 2** Inhibition constants for a panel of statin inhibitors.

Inhibitor	huCD <sup>a</sup> K <sub>i</sub> (nM)	SjCD IC <sub>50</sub> (nM)	SAP2 K <sub>i</sub> (nM)	Structure
P15C5	0.003	6	1.92	
P2	0.015	1.8	3.08	
P20	0.02	2.1	9.68	
P7	0.26	>1000	2.34	
P21	0.03	2.5	1.47	
MP-478A	0.18	2.3	6.87	
Pepstatin	0.01	4.6	1.37	

<sup>a</sup> Data for HuCD were taken from Majer et al. (1997) using Ac-Glu-Glu(EDANS)-Lys-Pro-Ile-Cys-Phe\*Phe-Arg-Leu-Gly-Lys(DABCYL)-Glu-NH<sub>2</sub> as substrate. Activities of SjCD and SAP2 were measured with human hemoglobin and Lys-Pro-Ala-Glu-Phe-nitroPhe-Ala-Leu as substrates, respectively (see materials and methods). Note the poor inhibition of SjCD with inhibitor P7, not observed with HuCD or SAP2.

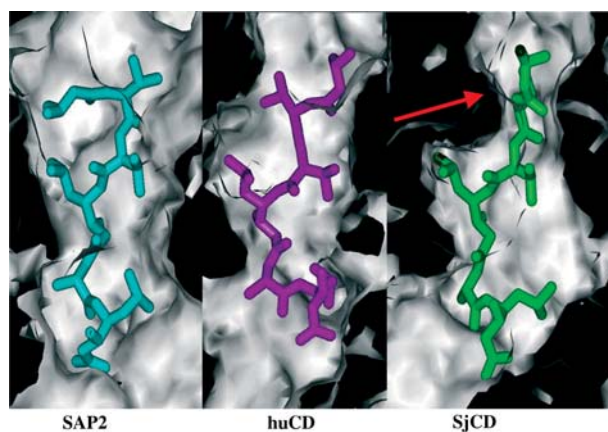


**Figure 4** A schematic view of the binding cavities of SAP2, huCD and SjCD.

A steric barrier (red arrow), not present in either SAP2 (left panel) or huCD (middle panel), is found encompassing the S2, S3 and S4 subsites of SjCD. The barrier in SjCD is composed mainly of the side chains of Met 224 and Phe 120. The C-terminus of pepstatin is at the bottom of each panel.

ortholog of the aspartic protease, cathepsin D, are important for this process and, as such, are considered potential targets for chemotherapeutic intervention (Caffrey et al., 2004).

As a source of SjCD for the inhibition data presented here, it would have been preferable to have either pure native or recombinant enzyme. However, insufficient quantities of native enzyme were obtainable from worms using pepstatin-agarose affinity chromatography. Also, attempts to produce recombinant enzyme in either *Escherichia coli* or *Pichia pastoris* were unsuccessful. Therefore, we used acidic worms extracts (SWE) that had been pre-treated with the cysteine protease inhibitor, E-64 [L-trans-L-leucylamido-(4-guanidino)butane], to select for aspartic protease activity (Caffrey et al., 1998). Other protease activities such as those due to serine or metallo-proteases are not detectable. However, the possibility of aspartic protease activities other than SjCD in SWE was considered. In the absence of annotated genomic sequence information, we queried the available *S. japonicum* expressed sequence tag (EST) database (Hu et al., 2003) with the term 'aspartic protease'. Of the approxi-

**Table 3** Geometrical parameters of pepstatin in different complexes with aspartic proteases.

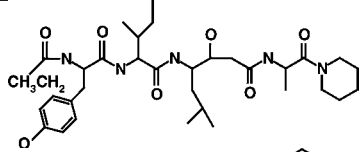
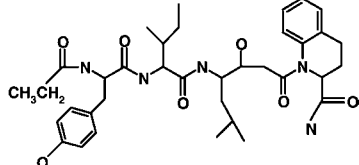
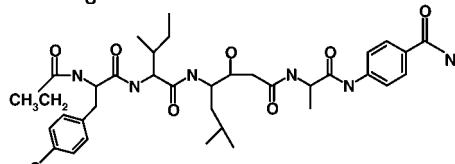
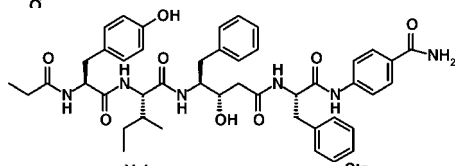
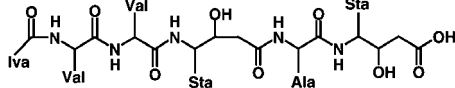
		Pepstatin angle (°)				
		Aspartic protease				
		1LYB cathepsin D	1PSO human pepsin	1QS8 plasmepsin	2RMP mucoropepsin	4ER2 endothiapepsin
1Iva	$\phi$	<b>-97.06</b>	<b>-177.25</b>	<b>-178.04</b>	<b>-128.52</b>	<b>-63.26</b>
	$\psi$	-135.95	-93.96	-114.94	-90.21	-126.12
2Val	$\omega$	-173.75	-158.82	179.67	-168.41	176.51
	$\phi$	<b>82.53</b>	<b>-91.80</b>	<b>-117.56</b>	<b>-134.80</b>	<b>-146.55</b>
3Val	$\psi$	113.63	132.93	135.97	102.21	132.19
	$\omega$	176.75	166.16	178.18	179.63	177.88
5Ala	$\phi$	-140.36	-125.33	-129.99	-104.42	-119.83
	$\psi$	115.21	98.88	106.99	126.31	99.84
4Sta	$\omega$	179.77	169.20	179.33	136.84	175.50
	$\phi$	-85.04	-68.42	-75.14	-69.18	-74.03
6Sta	$\psi$	<b>82.24</b>	<b>143.42</b>	<b>157.25</b>	<b>14.20</b>	<b>74.00</b>
	$\alpha$	<b>91.78</b>	<b>81.99</b>	<b>75.36</b>	<b>91.10</b>	<b>84.70</b>
	$\beta$	<b>71.25</b>	<b>75.61</b>	<b>76.71</b>	<b>76.81</b>	<b>85.59</b>
	$\gamma$	<b>68.57</b>	<b>63.67</b>	<b>62.71</b>	<b>62.76</b>	<b>59.50</b>
	$\delta$	<b>-131.20</b>	<b>-120.41</b>	<b>-127.19</b>	<b>-134.81</b>	<b>-123.41</b>
6Sta	$\zeta$	<b>-174.78</b>	<b>-173.57</b>	<b>-178.90</b>	<b>-178.55</b>	<b>-175.19</b>
	$\alpha$	<b>97.44</b>	<b>-102.13</b>	<b>-174.69</b>	<b>137.44</b>	<b>63.67</b>
	$\beta$	116.10	-81.24	-68.69	79.22	-179.58
	$\gamma$	20.70	85.72	108.08	100.60	56.92
	$\delta$	-102.47	-117.43	-158.36	-52.36	-104.51
	$\zeta$	<b>179.70</b>	<b>-174.08</b>	<b>-179.99</b>	<b>-177.89</b>	<b>175.32</b>

Values in bold italic face belong to the most flexible part of pepstatin. Values in bold face refer to the most rigid parts of pepstatin.

**Table 4** Root mean square deviation of pepstatins from different complexes compared to the reference complex 1LYB (human cathepsin D).

	Root mean square deviation			
	Enzyme			
	1PSO (pepsin)	1QS8 (plasmepsin)	2RMP (mucoropepsin)	4ER2 (endothiapepsin)
C <sub>α</sub> atoms	0.65	0.71	0.59	0.41
Backbone	1.04	1.08	1.18	0.78
Heavy atoms	1.79	1.95	1.99	1.17

**Table 5** Inhibition of SjCD, bovCD and SAP2 by second-generation statin inhibitors<sup>a</sup>.

Inhibitor	IC <sub>50</sub> (nM) <sup>a</sup>			Structure
	SjCD	bovCD	SAP2	
SJ1	140	40	32	
SJ2	15	80	68	
SJ3	60	100	46	
SJ4	30	15	58	
Pepstatin	0.06	1	–	

<sup>a</sup> Protease activity was measured with the peptidyl substrate 2-aminobenzoyl-Ile-Glu-Phe-nitroPhe-Arg-Leu-NH<sub>2</sub>.

mately 180 hits returned, all but four (i.e., >98%), encoded SjCD (L41346). The remaining ESTs encoded a second aspartic protease (accession numbers BU802603, BU798078, BU794016, and BU791797). Therefore, the inhibition assays detailed here are likely with respect to the predominant SjCD activity. We also checked the possibility of confounding co-factors in SWE, such as aspartic protease inhibitors, known to be present in other helminths (Martzen et al., 1991; Shaw et al., 2003). Querying the *S. japonicum* EST database with the term 'inhibitor' (to include the possibility of inhibitors of any enzyme) returned approximately 103 hits, many of which encoded inhibitors of serine, but not aspartic proteases. Also, querying the database by Blastn analysis with the pepsin inhibitors of *Ascaris suum* (Martzen et al., 1991) or *Trichostrongylus colubriformis* (Shaw et al., 2003) returned no hits. Accordingly, the presence of an aspartic protease inhibitor in SWE that exerted a significant influence on the quality of the data generated seems unlikely. Finally, and most importantly, the SAR results themselves indicate the reasonable homogeneity of the SWE aspartic protease activity. The lack of inhibition recorded for the P1–P3-bridged inhibitor, P7, relative to the other inhibitors (Table 2) was perfectly consistent with the demonstration by molecular modeling of a unique S2–S4 steric barrier in the SjCD binding site (Figure 4). Taken together, we conclude that SWE was of sufficient enzymatic homogeneity for the present study and an acceptable alternative to pure SjCD.

For any targeted therapy approach, it is necessary to have detailed information on the target enzyme's structure, in particular the topography, subsite composition,

and physical-chemical characteristics of the active site. With such information to hand, any particular substrate specificities can be clarified, thus facilitating rational drug design with small-molecule inhibitors. Ideally, a crystal structure for the target protease is required for such studies; however, none is available for the gut-associated schistosome proteases, including SjCD, the main subject of this report. Of necessity, therefore, determination of subsite specificities has relied on 3-D modeling based on the known crystal structure of an orthologous enzyme.

Homology modeling has been applied to the aspartic proteases of a number of blood-feeding parasites, including SjCD (Brinkworth et al., 2001) and its ortholog SmCD from *S. mansoni* (Silva et al., 2002). Both studies offered insight into the unusual specificity of these enzymes for cleavage at  $\alpha$ Phe36–Pro37 in human hemoglobin, a cleavage specificity not observed with human cathepsin D, but has been for HIV-1 protease (Darke et al., 1988) and the hookworm *Necator americanus* aspartic protease-2 (with canine hemoglobin only; Williamson et al., 2003). Thus, this unusual specificity of SjCD and SmCD might be exploited for design of selective anti-schistosomal compounds using scaffolds already employed for the synthesis of HIV-1 protease inhibitors (Silva et al., 2002)

Using the crystal structure of huCD-pepstatin as a template (Baldwin et al., 1993), we generated and compared a homology model of SjCD with huCD for active-site cleft topography and amino acid composition of subsites. HuCD is a well-described molecular system and various crystal structures are available at the PDB (1LYA, 1LYB, 1LYW) both complexed and uncomplexed.

The previous SjCD model generated by Brinkworth et al. (2001) served as a useful comparison with our model to ensure that both do not significantly deviate from one another. We found substantial agreement between both models, confirming the reliability of their independent construction.

As a further comparison and with a view to eventually designing selective inhibitors, we constructed a model of SAP2 from *Candida albicans*. Three-dimensional crystal structures of SAP2 and the closely related clinical isolate SAP2X, complexed with the potent inhibitor A-70450, have been reported (Stewart et al., 2001). Also, several analogues of A-70450 with potent SAP2X-inhibitory activity are known (Stewart et al., 2001). The details of how these compounds interact with the enzyme active site are not completely understood, although Pranav Kumar and Kulkarni (2002) showed that hydrogen bonding interactions were important for amino acid residues such as Gly-85, Asp-86, Asp-32, Asp-218, Tyr-225, and Ala-133. Also, significant hydrophobic interactions with the S3, S2, and S2' subsites contribute to the selectivity of these compounds. In our study, we confirmed the preferences for hydrophobic residue occupancy in the S3, S2, and S2' subsites. Overall, SAP2 has the broadest specificity of the three enzymes studied and this is as a consequence of possessing the largest binding cavity. Therefore, it can be envisaged that novel inhibitors of SjCD would also be effective against SAP2.

Our model of SjCD maintains important structural features present in the huCD-pepstatin crystal structure, namely, the overall fold, position of loops and active site residues in similar orientations. Optimization of SjCD with pepstatin revealed the sensitivity of the molecular mechanics, which can identify new orientations of side chains in mutated residues compared to those of huCD. In addition, we found that the binding cavity of SjCD has a number of subsite characteristics distinct from those of either huCD or SAP2. These are: (a) a different topology of active site loops, which would partially account for the different subsite specificities; (b) the S3 and S4 subsites in both huCD and SAP2 are more open than in SjCD; (c) SjCD lacks hydrogen bonding in the narrow S3 subsite, probably due to a lack of flexibility of pepstatin; and (d) the hydrogen bond network controlling conformation of the backbone of pepstatin in SjCD is missing in the SAP2-pepstatin complex. Finally, our modeling of different side chain rotamers in the subsites of SjCD identified a novel and major factor affecting the specificity of SjCD, i.e., a steric barrier between the S2, S3, and S4 subsites. This finding was supported by results of testing SjCD with a panel of inhibitors originally designed to map the specificity of huCD (Majer et al., 1997). One of these, P7, which contains a constraining P1–P3 bridge, showed inhibition at least three orders of magnitude weaker for SjCD than either huCD or SAP2.

Our identification of this steric barrier is of major importance for the future design of inhibitors with specificity for SjCD. Its presence was not detected by Brinkworth et al. (2001) probably because their modeling study focused on the cleavage specificities of peptidyl substrates rather than the testing of sterically constrained (bridged) inhibitors. Nonetheless, the geometrical para-

eters for subsites described by Brinkworth et al. (2001) accord with our findings. Therefore, their geometrical analyses are not inconsistent with our finding of a steric barrier.

We next utilized the SjCD model to screen *in silico* 20 suitable inhibitor chemistries that incorporate statin with a view to identifying novel inhibitors of increased specificity for SjCD. Screening efforts took into account the unique topographical, subsite composition and charge qualities of the active site of SjCD, not least the steric barrier between S2 and S4. The four inhibitors eventually selected, synthesized, and tested in substrate assays demonstrated low nanomolar inhibition values against SjCD, SAP2 and bovCD. Two of these were moderately more specific for SjCD than either SAP2 or bovCD. These first results, although modest, encourage further SAR studies and the four new inhibitors provide useful scaffolds for further optimization to increase both the sensitivity and selectivity of inhibitors for SjCD. A similar approach may also be adopted for SAP2 for which the prerequisite optimized model is described here.

## Materials and methods

### Molecular modeling

Sequence-to-structure alignment of the target and template proteins is the most important step in successful homology modeling (Miller et al., 2001). The crystal structure of huCD was the basis for the model of SjCD due to their reasonable homology (57.2% primary sequence identity). The crystal structure complexed with pepstatin (1LYB) was obtained from the PDB (Berman et al., 2000). Those amino acids of huCD differing from SjCD were mutated into their structural counterparts in the SjCD model using the Biopolymer module of the Insight II software package (Accelrys Inc., San Diego, USA). Numbering of SjCD corresponds to the huCD molecule as presented in 1LYB. There are two regions (90–101 and 316–318) longer in huCD than in SjCD and these were removed from the SjCD model. Also, the C-terminal extension of SjCD (see Figure 1) was not modeled. Both chains of huCD were united into one monomeric molecule to agree with the SjCD monomer. The same numbering system makes possible comparison of our model with that of Brinkworth et al. (2001).

The crystal structure of SAP2 in complex with the inhibitor A-70450 was also obtained from the PDB (ID: 1EAG). Although the structure of SAP2 in complex with pepstatin has been described (Cutfield et al., 1995), it is not yet available in the PDB. For the purposes of this study, it was necessary to replace A-70450 with pepstatin. Together with the model of SjCD constructed, the three proteases provide a unique ensemble of molecules sharing functional and structural similarity.

### Optimization of structural models

The details of the minimization protocol for all protease complexes are presented in Table 1. For SjCD, hydrogens were added to the system modeled from the huCD 1LYB structure, after which energetic minimization of the complex with pepstatin was performed. Computation utilized the Discover module from Accelrys Inc. with the AMBER force field (Cornell et al., 1995). First, the hydrogen atoms were optimized and consequently minimization of the complex with main chain atoms was attained. The last step was full minimization of the complex. The results of minimization were analyzed using the program Pro-



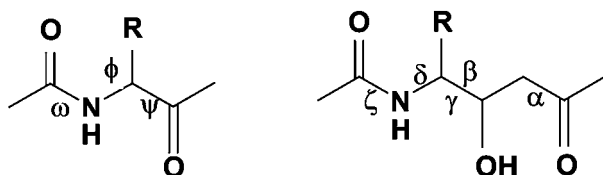


**Figure 5** Measured parameters of pepstatin in complexes with different aspartic proteases.

For constituent amino acid residues, the parameters are equivalent to the peptide bond torsion,  $\omega$ ,  $\phi$  and  $\psi$  – the torsions of the peptide backbone. For the statin scaffold the parameters are consequential torsions of the backbone  $\alpha$ ,  $\beta$ ,  $\gamma$ ,  $\delta$  and  $\zeta$ .

Check (Laskowski et al., 1993). Improper torsions and other discrepancies were corrected and the final minimization of the corrected model was repeated.

For SAP2, a similar protocol resulted in an optimized structure in complex with pepstatin. The only difference was that, in the initial step, the A-70450 inhibitor was replaced by pepstatin.

For huCD, the crystal structure of the enzyme in complex with pepstatin was minimized as for the SjCD and SAP2 models.

### Design of a specific SjCD inhibitor

For the design of a specific SjCD inhibitor, we used the pepstatin inhibitor scaffold for further optimization and characterized the binding modes of pepstatin across aspartic proteases families, in addition to the binding modes described here.

Pepstatin A was characterized in complex with a number of aspartic proteases (human pepsin: 1PSO; plasmepsin: 1QS8; mucoropepsin: 2RMP; endothiapepsin: 4ER2; plasmepsin II: 1SME and 1M43; plasmepsin IV: 1LS5) using molecular modeling. Our aim was to determine conformational flexibility and variability in binding modes. Different structures of pepstatin were superimposed and analyzed for differences in their topological parameters, e.g., binding and torsion angles, and conformations of side chains. Subsequently, pepstatin functional groups and distances from their interacting counterparts were characterized. The analyses of pepstatin parameters were based on the concept shown in Figure 5.

We compared a number of pepstatin and pepstatin-like inhibitors as a functional and structural core in different structural complexes (penicillopepsin with pepstatin and its analogues: 1APT, 1APU, 1APV, 1APW, and 1PPK; human cathepsin D: 1LYB; human pepsin: 1PSN and 1PSO; plasmepsin: 1QS8 and 1SME; *Rhizopus chinensis* hydrolase: 2APR, 3APR, and 4APR; endothiapepsin: 4ER2). The aims of these analyses were (i) to evaluate the binding modes of similar inhibitors in terms of their structural features and binding preferences in complex with different proteins and (ii) to find a general binding pattern belonging to the statin group of inhibitors. Structural searches were made in the ReliDatabase (Hendlich, 1998). We removed all ligands having a coefficient of 2D similarity with pepstatin of less than 0.7. Values of 2D similarity were calculated by the Tanimoto coefficient (Patterson et al., 1996), which describes topology by 'fingerprints' (on a scale of 0–1.0, where 1.0 means identity). The structures chosen were then compared with pepstatin.

The above analyses of different inhibitors in complex with a given protease or a single inhibitor in complex with different proteases should test our hypothesis that chosen inhibitors or their cores share similar conformations and binding patterns across the ensemble of aspartic protease complexes tested. The upper limit of contact distance between inhibitor and enzyme was chosen as 4.0 Å. In this range, we can identify hydrogen bonds and hydrophobic residues in mutual contact. Surfaces of enzyme subsites and inhibitors were visualized as Connolly surface plots and geometrical compatibilities of inhibitor and enzyme tested.

Analyses were evaluated based on the quantitative occupancy of amino acids residues in the subsites, the number of hydrogen bonds, and the mutual compatibility between amino acids of the inhibitor and enzyme.

### Inhibitor design

The results of the computer modeling of SjCD and structural analyses of the pepstatin-enzyme complexes produced a rational basis for the modification of statin-based inhibitors with special attention to their termini. Besides the subsite compatibility requirements, the design reflected the synthetic feasibility of any new inhibitors.

The 20 structures designed were chosen from a set of 100 structures based on the results of molecular modeling. We utilized the concept of an interaction energy calculation between protease and inhibitor. Holloway et al. (1995) suggested that, for structurally similar ligands, a correlation between interaction energy and  $K_i$  values, representing the Gibbs free energy, exists. Consequently, lower values of interaction energy for similar ligands (size and character) suggest higher affinity for the protease. The computational procedure included energy minimization of the designed inhibitors in different initial positions and the searching of up to three distinct conformers for each of the studied inhibitors inside the binding cavity. Finally, four inhibitors (Table 5) with the lowest interaction energies were selected for chemical synthesis and experimental measurement of inhibition values.

### Inhibitor synthesis

The non-natural amino acid Boc-Sta-OH was prepared according to the procedure of Jouin et al. (1987).

**Inhibitor SJ1** The peptide Prp-Tyr-Ile-Sta-Ala-OH was prepared via a Boc/Bzl strategy using a Merriemfield chlormethyl resin (1.3 mmol/g). Boc-Ala-OH was attached to the resin by the cesium salt method (degree of substitution 0.82 mmol Ala/g). The couplings were carried out with  $N,N'$ -diisopropylcarbodiimide (DIC)/1-hydroxybenzotriazole (HOBt) in dimethyl formamide (DMF). The peptide was cleaved with anhydrous HF in the presence of anisole as a scavenger. Crude lyophilized peptide was dissolved in DMF and added to a solution of piperidine (1.1 equivalents), (benzotriazol-1-yloxy)tris(di-methylamino)phosphonium hexa-fluorophosphate (BOP) (1.1 equivalents) and  $N,N$ -diisopropylethylamine (DIEA) (2.2 equivalents). After 6 h at room temperature, the mixture was evaporated and purified by preparative RP-HPLC.

FAB-MS,  $m/z$  (relative intensity, %): 646.7 (M+1, 100). Amino acid analysis: 1.0 Tyr, 1.0 Ile, 1.0 Ala.

**Inhibitors SJ2, SJ3 and SJ 4** These were prepared via a Boc/Bzl strategy using a  $p$ -methylbenzhydrylamine resin (1.3 mmol/g). The couplings were carried out with DIC/HOBt in DMF. The peptide was cleaved with anhydrous HF in the presence of anisole as a scavenger. Crude lyophilized peptides were purified by preparative RP HPLC.

SJ2: FAB MS,  $m/z$  (relative intensity, %): 697.7 (M+1, 100). Amino acid analysis: 1.0 Tyr, 1.0 Ile.

SJ3: FAB MS,  $m/z$  (relative intensity, %): 666.7 (M+1, 100). Amino acid analysis: 1.0 Tyr, 1.0 Ile, 1.0 Ala.

SJ4: FAB MS,  $m/z$  (relative intensity, %): 773.7 (M+1, 100). Amino acid analysis: 1.0 Tyr, 1.0 Ile, 1.0 Phe.

### Parasites

The life cycle of *S. japonicum* (strain form Hubei, PR China) was maintained as previously described (Ruppel et al., 1990). Adult

worms were perfused from NMRI mice and washed (3×10 min) in Dulbecco's modified Eagle medium (DMEM; Gibco Life Technologies, Eggenstein, Germany) containing 5% newborn calf serum (Gibco) and 0.05% heparin (2.5 U/ml; Braun, Melsungen, Germany). Following two further washes in the same medium without serum, worms were frozen in liquid nitrogen and stored for up to 8 months at -80°C.

### Preparation of *S. japonicum* soluble worm extract (SWE)

Worms (40 pairs) were disrupted by three freeze-thaw cycles followed by sonication (Branson sonifier B15) in 2.5 ml of 0.05 M sodium formate, pH 3.5. Sonication was carried out over an ice-cold water bath using a Branson Sonifier (10% duty cycle and output control 2). An initial pulse of 30 s was followed by 15 pulses each of 10 s and a final pulse of 30 s. The material was centrifuged for 20 min at 15 000 g and 4°C, and the supernatant (termed SWE) was removed, frozen in liquid nitrogen and stored at -80°C. The protein content of SWE was determined by microadaptation of the assay of Bradford (1976) using bovine serum albumin (fraction V; Serva, Heidelberg, Germany) as a standard protein.

### Preparation of bovCD

BovCD (a kind gift from M. Mares, Institute of Organic Chemistry and Biochemistry, Czech Academy of Sciences) was isolated from bovine spleen essentially according to Keilova and Tomasek (1976) using affinity chromatography on pepstatin-Sepharose as a final step.

### Purification of *Candida albicans* SAP2

SAP2 was purified as described by Pichova et al. (2001). Briefly, the *Candida*-conditioned medium was dialyzed against 15 mM sodium citrate, pH 5.6, applied to a DEAE-Sephadex A-25 column, and SAP2 was eluted with 100 mM sodium citrate, pH 5.6. The fractions containing active protease were pooled and used in inhibition assays.

### Determination of activity and inhibition of SjCD, bovCD and SAP2

**Assay with human hemoglobin** For tests of the initial panel of seven statin inhibitors (Table 2; Majer et al., 1997) with SjCD, human hemoglobin (Sigma, Deisenhofen, Germany) was used as the substrate as previously described (Caffrey et al., 1998). To a solution containing SWE (50 µl; 1.0–1.5 mg/ml) and 350 µl of sodium formate, pH 3.5, E-64 [5 µl in dimethyl sulfoxide (DMSO)] was added to a final concentration of 30 µM. E-64 was employed to eliminate cysteine protease activity known to be present in SWE (Caffrey et al., 1998). Following incubation for 15 min at 37°C, concentrations of aspartic protease inhibitor (5 µl in DMSO) ranging between 1 µM and 0.1 nM were added. After a further 15-min incubation period, hemoglobin was added (50 µl of a 4% solution) and the reaction was incubated for 2 h at 37°C. Linear reaction kinetics were recorded under these conditions. The reaction was stopped by precipitation with 450 µl of 10% trichloroacetic acid (TCA) and cooling on ice for 10 min. After centrifugation at 8800 g for 5 min, the TCA-soluble peptides in the supernatant were quantified by measurement of the absorbance at 280 nm in an Ultraspec II spectrophotometer (Amersham-Pharmacia, Freiburg, Germany). Reaction controls contained SWE that had been boiled for 15 min to inactivate all protease activity. Controls to account for the minor absorbances of inhibitors and solvent were also measured. As a blank, SWE followed by substrate and then buffer were added to ice-cold

10% TCA. The IC<sub>50</sub> value for inhibition by aspartic protease inhibitors was defined as that concentration of inhibitor required to inhibit the reaction by 50%.

**Assay with peptide substrates** For tests of the initial panel of seven statin inhibitors with SAP2 (Table 2), the chromogenic pepsin substrate Lys-Pro-Ala-Glu-Phe-nitroPhe-Ala-Leu was used as described previously (Pichova et al., 2001). SAP2 (1.5 nmol) was added to 1 ml of 100 mM sodium acetate, pH 3.3, containing 40 µM substrate and various concentrations of chosen inhibitors. Cleavage of substrate was monitored by measuring the decrease in absorbance at 300 nm on an Aminco DW 2000 spectrometer (SLM Instruments Inc., Rochester, USA).

For tests of second-generation statin inhibitors with SjCD, SAP2, and bovCD (Table 5), the chromogenic peptide, 2-aminobenzoyl-Ile-Glu-Phe-nitroPhe-Arg-Leu-NH<sub>2</sub> (synthesized at the Department of Biochemistry, Institute of Organic Chemistry and Biochemistry, Prague, Czech Republic), was employed as substrate (Brindley et al., 2001). The enzyme was preincubated with decreasing concentrations of inhibitors for 5 min at 37°C in 0.3 M sodium formate, pH 3.5, in a total volume 0.5 ml. The reaction was started by addition of 0.5 ml of 2.5 mM substrate (pre-warmed to 37°C) in 0.3 M sodium formate, pH 3.5. The absorbance at 305 nm was measured using a PU8800 spectrometer (Philips, Cambridge, UK).

### Acknowledgments

This work was supported by the Ministry of Education of the Czech Republic (grant no. LC512), Grant Agency of the Czech Republic 203/02/P095, GAVCR project A400550510. The Sandler Family Supporting Foundation and the United States National Institutes of Health grant AI 53247. It was also a part of research project Z4055905. C.R.C., J.K. and C.B. were recipients of a NATO Collaborative Linkage Grant (CLG 974914). We thank Andreas Ruppel (University of Heidelberg, Germany) for providing the *Schistosoma japonicum* worms and the reviewers for their detailed and helpful comments.

### References

- Baldwin, E.T., Bhat, T.N., Gulnik, S., Hosur, M.V., Sowder, R.C. II, Cachau, R.E., Collins, J., Silva, A.M., and Erickson, J.W. (1993). Crystal structures of native and inhibited forms of human cathepsin D: implications for lysosomal targeting and drug design. *Proc. Natl. Acad. Sci. USA* **90**, 6796–6800.
- Becker, M.M., Harrop, S.A., Dalton, J.P., Kalinna, B.H., McManus, D.P., and Brindley, P.J. (1995). Cloning and characterization of the *Schistosoma japonicum* aspartic proteinase involved in hemoglobin degradation. *J. Biol. Chem.* **270**, 24496–24501.
- Bein, M, Schaller, M, and Korting, HC. The secreted aspartic proteinases as a new target in the therapy of candidiasis. (2002). *Curr. Drug Targets* **3**, 351–357.
- Berman, H.M., Westbrook, J., Feng, Z., Gilliland, G., Bhat, T.N., Weissig, H., Shindyalov, I.N., and Bourne, P.E. (2000). The Protein Data Bank. *Nucleic Acids Res.* **28**, 235–242.
- Bradford, M.M. (1976). A rapid and sensitive method for the quantitation of microgram quantities of protein utilizing the principle of protein-dye binding. *Anal. Biochem.* **72**, 248–254.
- Brinkworth, R.I., Prociw, P., Loukas, A., and Brindley, P.J. (2001). Hemoglobin degrading, aspartic proteases of blood-feeding parasites. *J. Biol. Chem.* **276**, 38884–38851.
- Brindley, P.J., Kalinna, B.H., Wong, J.Y., Bogitsh, B.J., King, L.T., Smyth, D.J., Verity, C.K., Abbenante, G., Brinkworth, R.I., Fairlie, D.P. et al. (2001). Proteolysis of human hemoglobin

- by schistosome cathepsin D. *Mol. Biochem. Parasitol.* **112**, 103–112.
- Caffrey, C.R., Engel, A., Gsell, C., Göhring, K., and Ruppel, A. (1998). *Schistosoma japonicum* and *S. mansoni*: effect of cyclosporin A on aspartic and cysteine hemoglobinolytic activities. *Parasitol. Int.* **47**, 11–19.
- Caffrey, C.R., McKerrow, J.H., Salter, J.P., and Sajid, M. (2004). Blood 'n' guts: an update on schistosome digestive peptidases. *Trends Parasitol.* **20**, 241–248.
- Chitsulo, L., Loverde, P., and Engels, D. (2004). Schistosomiasis. *Nat. Rev. Microbiol.* **2**, 12–13.
- Cornell, W.D., Cieplak, P., Bayly, C.I., Gould, I.R., Merz Jr, K.M., Ferguson, D.M., Spellmeyer, D.C., Fox, T., Caldwell, J.W., and Kollman, P.A. (1995). A second generation force field for the simulation of proteins, nucleic acids, and organic molecules. *J. Am. Chem. Soc.* **117**, 5179–5197.
- Cutfield, S.M., Dodson, E.J., Anderson, B.F., Moody, P.C., Marshall, C.J., Sullivan, P.A., and Cutfield, J.F. (1995). The crystal structure of a major secreted aspartic proteinase from *Candida albicans* in complexes with two inhibitors. *Structure* **3**, 1261–1271.
- Darke, P.L., Nutt, R.F., Brady, S.F., Garsky, V.M., Ciccarone, T.M., Leu, C.T., Lumma, P.K., Freidinger, R.M., Veber, D.F., and Sigal, I.S. (1988). HIV-1 protease specificity of peptide cleavage is sufficient for processing of gag and pol polyproteins. *Biochem. Biophys. Res. Commun.* **156**, 297–303.
- Hendlich, M. (1998). Databases for protein-ligand complexes. *Acta Crystallogr. D Biol. Crystallogr.* **54**, 1178–1182.
- Higgins, D., Thompson, J., Gibson, T., Thompson, J.D., Higgins, D.G., and Gibson, T.J. (1994). CLUSTAL W: improving the sensitivity of progressive multiple sequence alignment through sequence weighting, position-specific gap penalties and weight matrix choice. *Nucleic Acids Res.* **22**, 4673–4680.
- Holloway, M.K., Wai, J.M., Halgren, T.A., Fitzgerald, P.M., Vacca, J.P., Dorsey, B.D., Levin, R.B., Thompson, W.J., Chen, L.J., and deSolms, S.J. (1995). *A priori* prediction of activity for HIV-1 protease inhibitors employing energy minimization in the active site. *J. Med. Chem.* **38**, 305–317.
- Hu, W., Yan, Q., Shen, D.K., Liu, F., Zhu, Z.D., Song, H.D., Xu, X.R., Wang, Z.J., Rong, Y.P., Zeng, L.C., et al. (2003). Evolutionary and biomedical implications of a *Schistosoma japonicum* complementary DNA resource. *Nat. Genet.* **35**, 139–147.
- Jouin, P., Castro, B., and Nisato, D. (1987). Stereospecific synthesis of N-protected statine and its analogs via chiral tetramic acid. *J. Chem. Soc. Perkin Trans. T1* **6**, 1177–1182.
- Keilova, H. and Tomasek, V. (1976). Isolation and some properties cathepsin D inhibitor from potatoes. *Collect. Czech. Chem. Commun.* **41**, 487–497.
- Laskowski, R.A., MacArthur, M.W., Moss, D.S., and Thornton, J.M. (1993). PROCHECK: a program to check the stereochemical quality of protein structures. *J. Appl. Cryst.* **26**, 283–291.
- Majer, P., Collins, J.R., Gulnik, S.V., and Erickson, J.W. (1997). Structure-based subsite specificity mapping of human cathepsin D using statin-based inhibitors. *Protein Sci.* **6**, 1458–1466.
- Martzen, M.R., McMullen, B.A., Fujikawa, K., and Peanasky, R.J. (1991). Aspartic protease inhibitors from the parasitic nematode *Ascaris*. *Adv. Exp. Med. Biol.* **306**, 63–73.
- Miller, M., Ginalski, K., Lesyng, B., Nakaigawa, N., Schmidt, L., and Zbar, B. (2001). Structural basis of oncogenic activation caused by point mutations in the kinase domain of the MET proto-oncogene: modeling studies. *Proteins* **44**, 32–43.
- Patterson, D.E., Cramer, R.D., Ferguson, A.M., Clark, R.D., and Weinburger, L.E. (1996). Neighborhood behavior: a useful concept for validation of 'molecular diversity' descriptors. *J. Med. Chem.* **39**, 3049–3059.
- Pearce, E.J., and MacDonald, A.S. (2002). The immunobiology of schistosomiasis. *Nat. Rev.* **2**, 499–511.
- Pichova, I., Pavlickova, L., Dostal, J., Dolejsi, E., Hruskova-Heidingsfeldova, O., Weber, J., Ruml, T., and Soucek, M. (2001). Secreted aspartic proteases of *Candida albicans*, *Candida tropicalis*, *Candida parapsilosis* and *Candida lusitanae*. Inhibition with peptidomimetic inhibitors. *Eur. J. Biochem.* **268**, 2669–2677.
- Pranav Kumar, S.K. and Kulkarni, V.M. (2002). Insights into the selective inhibition of *Candida albicans* secreted aspartyl protease: a docking analysis study. *Bioorg. Med. Chem.* **10**, 1153–1170.
- Ruppel, A., Shi, Y.E., and Moloney, N.A. (1990). *Schistosoma mansoni* and *S. japonicum*: comparison of levels of ultraviolet irradiation for vaccination of mice with cercariae. *Parasitology* **101**, 23–26.
- Shaw, R.J., McNeill, M.M., Maass, D.R., Hein, W.R., Barber, T.K., Wheeler, M., Morris, C.A., and Shoemaker, C.B. (2003). Identification and characterisation of an aspartyl protease inhibitor homologue as a major allergen of *Trichostrongylus colubriformis*. *Int. J. Parasitol.* **33**, 1233–1243.
- Silva, F.P. Jr., Ribeiro, F., Katz, N., and Giovanni-De-Simone, S. (2002). Exploring the subsite specificity of *Schistosoma mansoni* aspartyl hemoglobinase through comparative molecular modelling. *FEBS Lett.* **514**, 141–148.
- Stewart, K. and Abad-Zapatero, C. (2001). *Candida* proteases and their inhibition: prospects for antifungal therapy. *Curr. Med. Chem.* **8**, 941–448.
- Vondrasek, J. and Wlodawer, A. (1998). Inhibitors of HIV-1 protease: a major success of structure-assisted drug design. *Annu. Rev. Biophys. Biomol. Struct.* **27**, 249–284.
- Wasilewski, M.M., Lim, K.C., Phillips, J., and McKerrow, J.H. (1996). Cysteine protease inhibitors block schistosome hemoglobin degradation *in vitro* and decrease worm burden and egg production *in vivo*. *Mol. Biochem. Parasitol.* **81**, 179–189.
- Williamson, A.L., Brindley, P.J., Abbenante, G., Datu, B.J., Proci, P., Berry, C., Girdwood, K., Pritchard, D.I., Fairlie, D.P., Hotez, P.J., Zhan, B., and Loukas, A. (2003). Hookworm aspartic protease, Na-APR-2, cleaves human hemoglobin and serum proteins in a host-specific fashion. *J. Infect. Dis.* **187**, 484–494.